Bone Reports 10 (2019) 100205

Contents lists available at ScienceDirect

Bone Reports

journal homepage: www.elsevier.com/locate/bonr

Adenoviral mediated mono delivery of BMP2 is superior to the combined delivery of BMP2 and VEGFA in bone regeneration in a critical-sized rat calvarial bone defect

Sunita Sharma[a,*], Ying Xue[a], Zhe Xing[a], Mohammed A. Yassin[b], Yang Sun[b], James B. Lorens[c], Anna Finne-Wistrand[b], Dipak Sapkota[d], Kamal Mustafa[a,*]

[a] Department of Clinical Dentistry, Faculty of Medicine, University of Bergen, Bergen, Norway
[b] Department of Fibre and Polymer Technology, KTH Royal Institute of Technology, Stockholm, Sweden
[c] Department of Biomedicine, University of Bergen, Bergen, Norway
[d] Department of Oral Biology, Faculty of Dentistry, 0316 Oslo, Norway

ARTICLE INFO

Keywords:
Bone tissue engineering
Copolymer scaffold
Mesenchymal stem cells
MicroCT

ABSTRACT

Apart from osteogenesis, neovascularization of the defect area is an important determinant for successful bone healing. Accordingly, several studies have employed the combined delivery of VEGFA and BMP2 for bone regeneration. Nevertheless, the outcomes of these studies are highly variable. The aim of our study was to compare the effectiveness of adenoviral mediated delivery of BMP2 alone and in combination with VEGFA in rat bone marrow stromal cells (rBMSC) seeded on a poly(LLA-*co*-CL) scaffold in angiogenesis and osteogenesis using a critical-sized rat calvarial defect model. Both mono delivery of BMP2 and the combined delivery of a lower ratio of VEGFA and BMP2 (1:4) led to up-regulation of osteogenic genes (*Alpl* and *Runx2*) and increased calcium deposition *in vitro*, compared with the GFP control. Micro computed tomography (microCT) analysis of the rat calvarial defect at 8 weeks showed that the mono delivery of BMP2 (43.37 ± 3.55% defect closure) was the most effective in healing the bone defect, followed by the combined delivery of BMP2 and VEGFA (27.86 ± 2.89%) and other controls. Histological and molecular analyses supported the microCT findings. Analysis of the angiogenesis, however, showed that both mono delivery of BMP2 and combined delivery of BMP2 and VEGFA had similar angiogenic effect in the calvarial defects. Examination of the key genes related to host response against the adenoviral vectors showed that the current model system was not associated with adverse immune response. Overall, the results show that the mono delivery of BMP2 was superior to the combined delivery of BMP2 and VEGFA in healing the critical-sized rat calvarial bone defect. These findings underscore the importance of appropriate growth factor combination for the successful outcome in bone regeneration.

1. Introduction

The autologous bone graft, although considered the gold standard for the treatment of large bone defects, is unable to meet the current increased need for bone grafting (Fillingham and Jacobs, 2016). Moreover, the procedure has a number of drawbacks, such as donor site morbidity, leading to prolonged hospital admissions and higher associated costs, unpredictable healing and resorption (Fillingham and Jacobs, 2016; Younger and Chapman, 1989). In this context, bone tissue engineering (BTE) approach is rapidly evolving as a promising alternative to the autologous bone grafting procedures. For successful outcome in BTE, selection of appropriate osteoinductive and/or angiogenic growth factors, a suitable delivery method and a proper supportive scaffold are critical. Additionally angiogenesis is cruical for the survival and the integration of BTE construct and effective bone healing. In an attempt to dev elop an effective model system for BTE, we previously investigated adenoviral-mediated delivery of bone morphogenetic protein 2 (BMP2) and vascular endothelial growth factor A (VEGFA) alone or in combination in human bone marrow stromal cells (BMSC) seeded onto a biodegradable and well characterized copolymer poly(L-lactide-*co*-ϵ-caprolactone) (poly(LLA-*co*-CL)) scaffold (Sharma et al., 2016). The careful selection of poly(LLA-*co*-CL) scaffold for this model system was based on our previous findings, that this scaffolding material has optimal biophysical features (Dånmark et al., 2011; Odelius et al., 2005), such as surface characteristics and biocompatibility (Xue et al., 2010; Xing et al., 2011; Idris et al., 2010) for BTE.

* Corresponding authors.
E-mail addresses: drsunitaaz@gmail.com (S. Sharma), kamal.mustafa@uib.no (K. Mustafa).

https://doi.org/10.1016/j.bonr.2019.100205
Received 2 November 2018; Received in revised form 11 March 2019; Accepted 10 April 2019
Available online 11 April 2019

Additionally, the adenoviral mediated gene delivery method used in this model minimizes the disadvantages (such as rapid degradation, requirement of supraphysiological doses and unpredictable adverse effects, and high cost) associated with the bulk delivery of recombinant growth factors at the defect site (Evans, 2012).

In a previous study using a subcutaneous mouse model (ectopic) system, we showed that adenoviral-mediated delivery of BMP2 in BMSC seeded onto poly(LLA-*co*-CL) scaffolds was feasible and effective in angiogenesis and bone regeneration (Sharma et al., 2016). Further, we demonstrated that although BMSC expressing VEGFA alone, or in combination with BMP2 significantly induced angiogenesis, VEGFA alone failed to demonstrate osteogenic activity both *in vitro* and *in vivo* in a subcutaneous mouse model as compared to the combined delivery group (Sharma et al., 2018). Even in the combined delivery group, the VEGFA appears not to provide any additional effect over the BMP2 in bone regeneration (Sharma et al., 2016; Sharma et al., 2018). These findings prompted us to exclude the delivery of VEGFA alone in the current study. The current study aimed to examine and translate the findings of our previous work in a more clinically relevant critical-sized rat calvarial bone defect model and to compare the role of BMP2 alone and in combination with VEGFA (VEGFA:BMP2 = 1:4) in angiogenesis and in bone formation, at both molecular and functional levels.

2. Materials and methods

2.1. Rat BMSC (rBMSC) isolation and culture

rBMSCs were isolated from 6-week old male Lewis rats as previously described (Xing et al., 2011; Maniatopoulos et al., 1988). Briefly, after 1 week of acclimatization, four animals were euthanized by carbon dioxide (CO_2) inhalation and cervical dislocation. The femurs were removed and carefully scrubbed to remove soft tissues and washed with phosphate buffered saline (PBS) supplemented with 3% antibiotic-antimycotic (Gibco, Life technologies). The metaphyseal ends of the femurs were excised and the marrow cavity was flushed with complete minimum essential medium (αMEM, Invitrogen, Carlsbad, California, USA) to collect the bone marrow cells into a sterile falcon tube. The isolated cells were centrifuged and suspended in fresh α-MEM medium containing 1% penicillin-streptomycin, 15% FBS and 1% glutamax, and plated in culture flasks. The following day, unattached cells were discarded and the medium was replaced with fresh αMEM medium containing 1% glutamax, 1% penicillin-streptomycin and 10% FBS. The cells were sub-cultured at day 3 when they appeared spindle-shaped and had reached 80–90% confluence. The Norwegian Animal Research Authority approved the animal experiment (local approval number 20146703) and all animal experiments were conducted in accordance to the European Convention for the Protection of Vertebrates.

2.2. Preparation of rBMSC seeded scaffolds

Porous poly(LLA-*co*-CL) scaffolds were fabricated using the solvent-casting particulate-leaching method as described previously (Odelius et al., 2005; Danmark et al., 2010). For *in vitro* experiments, scaffolds (diameter ≈ 12 mm, height ≈ 1.3 mm, porosity: 85% and average pore size: 90–500 μm as determined by microcomputed tomography) were placed on the bottom of 48-well plates, pre-wetted with the culture medium and incubated overnight at a humidified atmosphere at 37 °C and 5% CO_2. rBMSC were seeded at a density of 1×10^5 cells/scaffold.

2.3. Adenoviral expression vector construction and transduction of rBMSC

In the current study, we used adenoviral mediated expression constructs for human BMP2 and VEGFA as previously used in our studies (Sharma et al., 2016; Sharma et al., 2018). A high level of sequence homology has been reported between human and rat BMP2 (Freire et al., 2012; Freire et al., 2015) and VEGFA (Avivi et al., 1999; Ferrara, 2002) proteins, and accordingly in many studies human recombinant BMP2 and VEGFA have been used successfully in bone regeneration experiments in the rat (Park et al., 2003; Li et al., 2016). Replication-deficient adenoviral expression vectors carrying the coding sequences of *VEGF165* (reference sequence: NM_001025370.2) (ad-VEGFA) and *BMP2* gene (reference sequence: NM_001200.2) (ad-BMP2) were purchased from Cyagen Biosciences Inc. In the ad-VEGFA, gene encoding for *DsRed* was used as a marker, and in the ad-BMP2 construct, gene encoding for enhanced green fluorescent protein (eGFP) was used. The adenoviral vector carrying only *eGFP* coding sequences (ad-GFP) was used as a control. Adenoviral particles were generated by transfecting HEK 293 cells (ATCC-CRL-1573) with *Pac* I digested constructs. Early passage (passage 2–3) BMSC were infected as monolayer cultures with respective adenoviruses (multiplicity of infection, MOI = 100) to obtain 80–90% infection efficiency as disclosed by fluorescent microscopy. Rat BMSC were infected with ad-GFP, ad-BMP2 and a mixture of ad-VEGFA + BMP2 (20 MOI VEGFA + 80 MOI BMP2; ratio 1:4) and are henceforth be referred to as 'ad-GFP', 'ad-BMP2' and 'ad-BMP2 + VEGFA' respectively. After 48 h of infection in monolayer culture with the respective adenoviral particles, rBMSC were seeded onto poly(LLA-*co*-CL) scaffolds. rBMSC grown in scaffolds and the respective conditioned media were harvested after 3 and 14 days for mRNA analyses and ELISA assay respectively.

2.4. Total RNA extraction

Total RNA from the *in vitro* seeded scaffolds and the *in vivo* calvarial explants were extracted using Maxwell® 16 LEV simplyRNA Kit (Cat no: AS1270, Promega) on a Maxwell® 16 instrument following the manufacturer's protocol. The quantity and purity of total RNA were determined using a Nanodrop Spectrophotometer (ThermoScientific Nano Drop Technologies, Wilmington, DE, USA). The integrity of RNA was examined by using Agilent 2100 Bioanalyzer (Agilent Technologies).

2.5. Reverse transcription and quantitative RT-PCR (qRT-PCR) using TaqMan assays

Three hundred nanograms of total RNA were converted to cDNA by reverse transcription reaction using a high capacity cDNA Archive Kit (Applied Biosystems, Carlsbad, CA, USA). *VEGFA* (Hs00900055_m1) and *BMP2* (Hs00154192_m). TaqMan assays were used to verify the expression of human *VEGFA* and *BMP2* mRNA in adenovirus transduced rBMSC. The following TaqMan assays were used to amplify mRNAs from rBMSC seeded onto scaffolds (*in vitro*) or rat calvarial explants *in vivo*: *Bmp2* (Rn00567818_m1), *Vegfa* (Rn01511601_m1), *Alpl* (Rn01516028_m1), *Runx2* (Rn01512298_m1), *Spp1* (Rn00681031_m1), *Ostf1* (Rn00686607_m1), *Ifna1* (Rn02395770_g1), *Infb1* (Rn00569434_s1), *Il1a* (Rn00566700_m1) and *Il1b* (Rn00580432_m1). *Gapdh* (Rn01749022_g1) was used as an endogenous control. All qRT-PCR amplifications were performed on ABI Prism Sequence Detector 7900 HT (Applied Biosystems, Foster City, USA) under standard cycling conditions. Comparative $2^{-\Delta\Delta Ct}$ method was used to quantify the relative mRNA expression.

2.6. Alkaline phosphatase (ALP) staining

ALP staining was used to analyze the osteoblastic differentiation potential of rBMSC transduced with the respective adenoviral particles. After 48 h of infection, cells were trypsinized and 2×10^4 cells were seeded in monolayers on 4-well culture dishes. ALP staining was done on day 3 and 14. Briefly, cells were washed with PBS, fixed and stained for ALP activity using SigmaFast™ BCIP/NBT (Sigma-Aldrich). The staining intensity of captured images was quantified using ImageJ software (1.5 versions for mac) using 8 bit gray scale images. The assay was repeated at least three times.

2.7. Alizarin red staining (in vitro mineralization assay)

To assess *in vitro* mineralization, Alizarin red staining was performed on rBMSC from different experimental groups cultured as monolayers as well as in poly(LLA-*co*-CL) scaffolds on day 21. Briefly, after carefully washing with the Dulbecco's PBS, the cells grown in monolayer culture and in scaffolds were fixed with 4% paraformaldehyde for 10 min. Thereafter, the cells were stained with 2% Alizarin red S staining solution (Sigma-Aldrich), incubated for 45 min, washed, visualized and imaged under a light microscope.

2.8. Rat BMP2 ELISA

Culture supernatants from the transduced rat BMSC seeded onto scaffolds were collected at 3 and 14 days for ELISA analysis of rat BMP2 (Cat no: KA0541, Abnova). ELISA assay was performed in duplicates following the manufacturer's instructions.

2.9. In vivo critical-sized calvarial bone defect model in Lewis rat

2.9.1. Preparation of scaffold implants

Poly(LLA-*co*-CL) scaffolds (diameter ≈ 5 mm, height ≈ 1.3 mm, porosity: 85% and average pore size: 90–500 μm as determined by microcomputed tomography) were placed on the bottom of 96-well plates, pre-wetted with the culture medium and incubated overnight at a humidified atmosphere of 37 °C and 5% CO_2. After 48 h of infection in monolayer culture with the respective adenoviral particles, 1×10^6 rat BMSC were seeded onto each scaffold. To facilitate uniform cell distribution from the scaffold surface into the internal pores, culture plates were gently shaken on an orbital shaker (Eppendorf, Germany) at 500 rpm for 5 min. The scaffolds seeded with cells were incubated for a further 3 h to allow cell attachment, and thereafter implanted into the calvarial bone defects in Lewis rats. Scaffolds without any rBMSC (scaffold only) were used as negative controls in the *in vivo* experiments.

2.9.2. Surgical implantation of scaffolds

Thirty-four male Lewis rats (12 weeks old) (17 rats each for the 2 and 8 week time-points) were used for scaffold implantation in the calvarial defect. The animals were anesthetized with sevoflurane (SevoFlo, Aesica Queenborough Limited, United Kingdom) in combination with air and O2. A surgical site extending from the bridge of the snout between the eyes to the caudal end of the calvarium was prepared by shaving the hair and scrubbing with the alcohol. An approximately 2 cm long midline sagittal incision was made, the periosteum covering the calvarium was divided by an incision down the sagittal midline, and the periosteum was gently pushed laterally while elevating it from the underlying skull using an elevator. A saline-cooled trephine drill was used to create two defects of 5 mm diameter in each parietal bone, carefully protecting the dura mater. The defects were randomly filled with scaffolds containing one of the following groups of rBMSC (8 replicates for each group for both 2 and 8 week time-points): i) ad-GFP, ii) ad-BMP2, iii) ad-BMP2 + VEGFA or iv) untransduced. Scaffolds without any cells (scaffold only group) were used as negative controls. The incisions were closed with 4–0 vicryl sutures. The animals were given a subcutaneous analgesic dose of Buprenorphine (Temgesic 0.3 mg/kg). The animals were monitored daily for condition of the surgical wound, animal activity, food intake, and any signs of infection. Animals were euthanized with CO_2 inhalation and subsequent cervical dislocation at 2 and 8 weeks. Five of the scaffolds from each experimental group at 2 week time point were cut into two halves and used for i) RNA extraction (stored in RNA later, Ambion), and ii) cryosection (embedded in Tissue-Tek). The remaining 3 scaffolds from each group were fixed in 4% buffered formalin for 24 h, scanned using micro computed tomography (microCT), decalcified in 12.5% EDTA and 2.5% PFA in phosphate buffered saline for 7–10 days, and embedded in paraffin. At 8 weeks, all of the scaffolds from each group were formalin fixed, scanned using microCT, decalcified and embedded in paraffin for histological analysis.

2.10. Histological analysis

The formalin fixed and paraffin embedded specimens were cut into 5 μm sections. The sections were deparaffinized in xylene, rehydrated in graded ethanol and stained with Hematoxylin and Eosin or Masson's trichrome stain. Vascularity in the implanted scaffolds was quantified in Masson's trichrome stained slides by counting the pink/red stained capillaries/blood vessels containing brown/orange stained erythrocytes. Briefly, at least three randomly selected areas per slide including the periphery and interior of the scaffold explants were used to count the capillaries/blood vessels using digitally scanned slides (20×; Nano Zoomer XR digital scanner, Hamamatsu).

2.11. Micro computed tomography analysis (microCT)

The *in vivo* scaffold explants harvested at 2 and 8 weeks were scanned with a Sky Scan 1172 X-ray μCT imaging system (Kontich, Belgium) to visualize the 3D distribution and volume of mineralized tissue. Samples were scanned with an X-ray source of 60 kV/200 μA, a 0.5 mm aluminum filter for a 10 μm resolution, and a 0.4° rotation step. The projection image was reconstructed using NRecon ReconstructionVR (v. 1.6.10) software. The quantitative analysis of the image was performed by CTan software (v.1.15, Skyscan, Belgium). A global threshold of 90–255 was applied to all the samples after determining the standardized cylindrical Volume of Interest (VOI), 5 mm in diameter and 1.3 mm in height. Data were reported as the percentage binarized object volume measured within this VOI. Bone volume (BV), tissue volume (TV), and BV/TV ratios were recorded.

2.12. Statistical analyses

Data are expressed as mean ± standard error of the mean (SEM). ANOVA test with Bonferroni *post hoc* analysis was used for comparison of the means between multiple groups. Statistical analyses were performed using GraphPad Prism software version 5.00 for Windows (GraphPad Software, San Diego California USA, www.graphpad.com), with the level of significance set at 5%.

3. Results

3.1. BMP2 and VEGFA adenoviral expression vectors up-regulated respective human and rat specific mRNAs in rBMSC

ad-BMP2 and ad-BMP2 + VEGFA rBMSC seeded in poly(LLA-*co*-CL) scaffolds expressed significantly higher levels of human *BMP2* mRNA level at days 3 and 14, compared with the control ad-GFP rBMSC (Fig. 1A and E). Similarly, significantly higher levels of human *VEGFA* mRNA were found in ad-VEGFA + BMP2 group at day 3 and 14, compared with the control ad-GFP and ad-BMP2 groups (Fig. 1B and F). It should be noted that expression of *BMP2* mRNA was lower in ad-BMP2 + VEGFA group than in the ad-BMP2 group (Fig. 1A and E). We next examined whether ad-BMP2 and ad-VEGFA constructs had any influence on the expression of endogenous rat *Bmp2* and *Vegfa* mRNA levels in the rBMSC. Indeed, ad-BMP2 and ad-VEGFA constructs respectively led to increased expression of rat *Bmp2* and *Vegfa* mRNA and secreted rat BMP2 protein both at day 3 and day 14 (Fig. 1C, D and G–J). However, the BMP2 and VEGFA adenoviral vector mediated induction of rat *Bmp2* and *Vegfa* mRNA levels were not as pronounced as that of the corresponding human mRNAs (Fig. 1A–H).

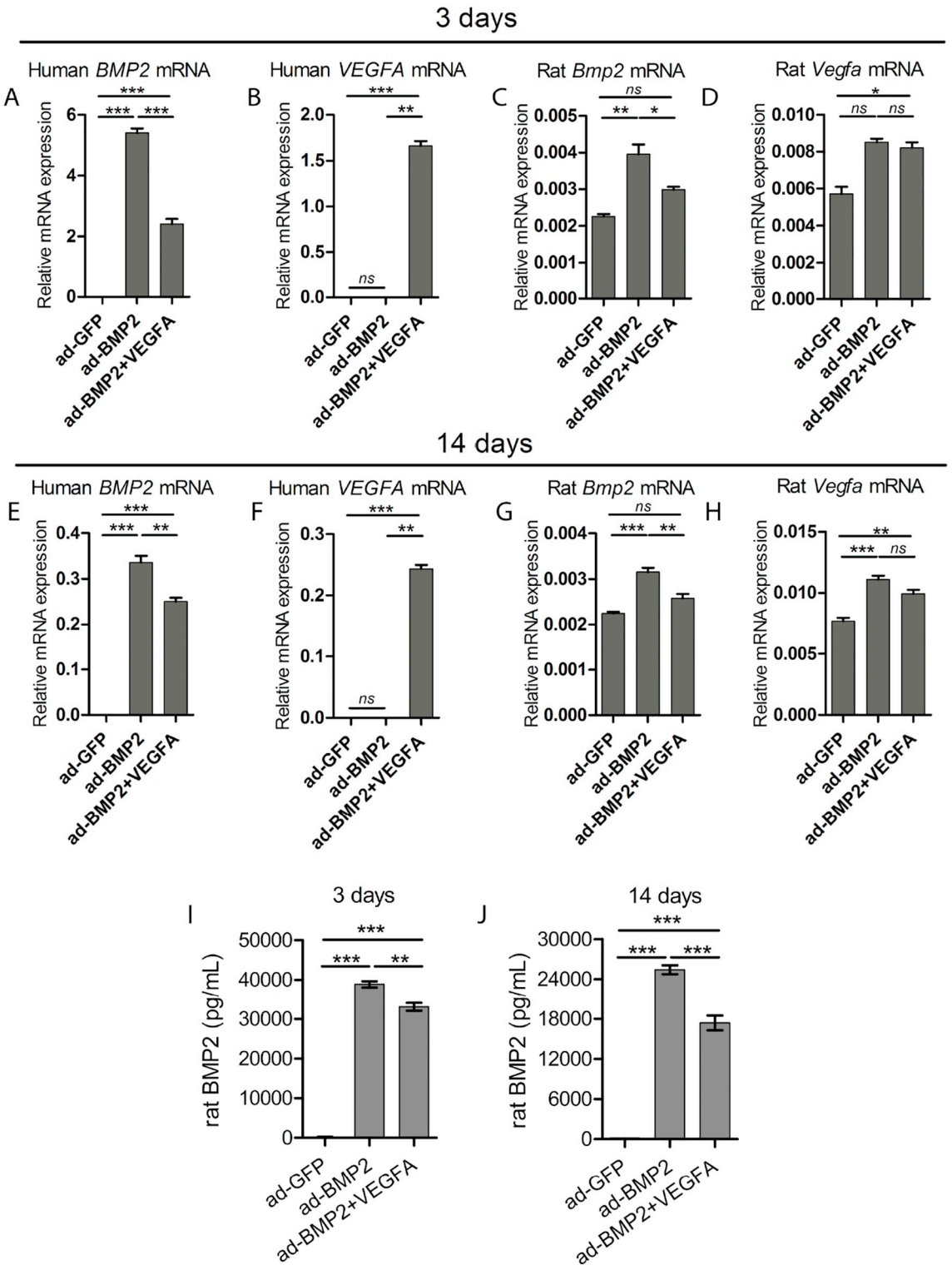

Fig. 1. VEGFA and BMP2 adenoviral expression vectors respectively increased expression of both human and rat specific mRNA levels in rBMSC.
Significant up-regulation of human and rat specific *BMP2* mRNA (A, C, E and G) and secreted BMP2 protein (I and J) levels were found at day 3 and 14 in both ad-BMP2 and ad-BMP2 + ad-VEGFA groups, compared with the ad-GFP group. Similarly, significant up-regulation of human and rat specific *VEGFA* mRNA (B, D, F and H) was found in ad-BMP2 + VEGFA group, compared with the ad-GFP and ad-BMP2 groups at both time points. mRNA expression levels of *Gapdh* were used to normalize the data. (I and J) Higher levels of secreted rat specific BMP2 protein were found in the culture supernatant of ad-BMP2 and ad-BMP2 + VEGFA groups by using ELISA assay at 3 and 14 days. The error bars in (A–H) represent SEM of 3 biological replicates ($n = 3$) done in 3 technical replicates. The error bars in (I–J) represent SEM of 3 biological replicates ($n = 3$) done in duplicates. ANOVA test with Bonferroni *post hoc* analysis was used for statistical analysis in (A–J). ***, $p < 0.001$; **, $p = 0.001$–0.01; *, $p = 0.01$–0.05; ns, non-significant.

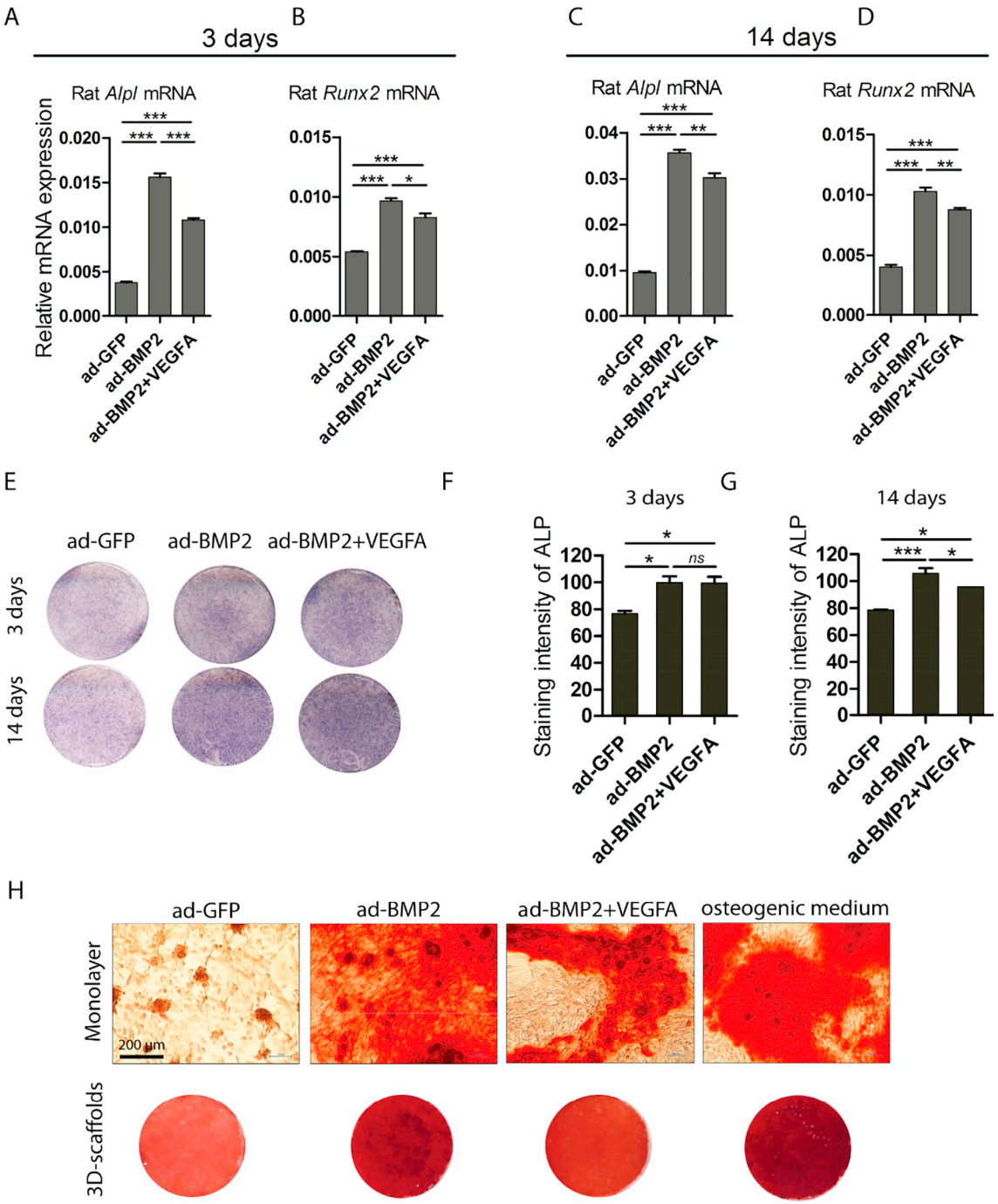

Fig. 2. Adenoviral vector mediated expression of BMP2 alone and in combination with VEGFA led to up-regulation of osteogenic molecules *in vitro*. Significantly higher mRNA levels of *Alpl* and *Runx2* were found in ad-BMP2 and ad-BMP2 + VEGFA groups at both time points (A–D). The error bars represent SEM of 3 biological replicates ($n = 3$) done in 3 technical replicates. (E) Representative images and quantification (F and G) demonstrating higher alkaline phosphatase activity in ad-BMP2 and ad-BMP2 + VEGFA groups in monolayer culture, compared with the ad-GFP group at 3 and 14 days. Experiments were repeated at least three times. ANOVA test with Bonferroni *post hoc* analysis was performed for statistical analysis in A–D, F and G. ***, $p < 0.001$; **, $p = 0.001$–0.01; *, $p = 0.01$–0.05; ns, non-significant. (H) Significantly higher amount of calcium deposition was found in ad-BMP2 and ad-BMP2 + VEGFA groups both in monolayer culture and in poly(LLA-*co*-CL) scaffold, compared with the ad-GFP group on 21 days. rBMSC grown in osteogenic medium was used as a positive control. The experiments were repeated at least three times.

3.2. Adenoviral mediated delivery of BMP2 alone and in combination with VEGFA was associated with up-regulation of rat specific osteogenic markers and increased calcification in vitro

Ad-BMP2 and ad-BMP2 + VEGFA rBMSC seeded onto poly(LLA-*co*-CL) scaffolds expressed significantly higher levels of *Alpl* and *Runx2*, compared with the ad-GFP rBMSC both at 3 and 14 days (Fig. 2A–D). In parallel, ALP activity significantly increased at 3 and 14 days in both ad-BMP2 and ad-BMP2 + VEGFA groups, compared with the ad-GFP control group (Fig. 2E–G). These molecular changes were paralleled functionally as demonstrated by the Alizarin red staining (Fig. 2H), where significantly more calcium deposition was observed in ad-BMP2 and ad-BMP2 + VEGFA rBMSC grown in monolayer and in poly(LLA-*co*-CL) scaffolds, compared with the ad-GFP rBMSC. However, the

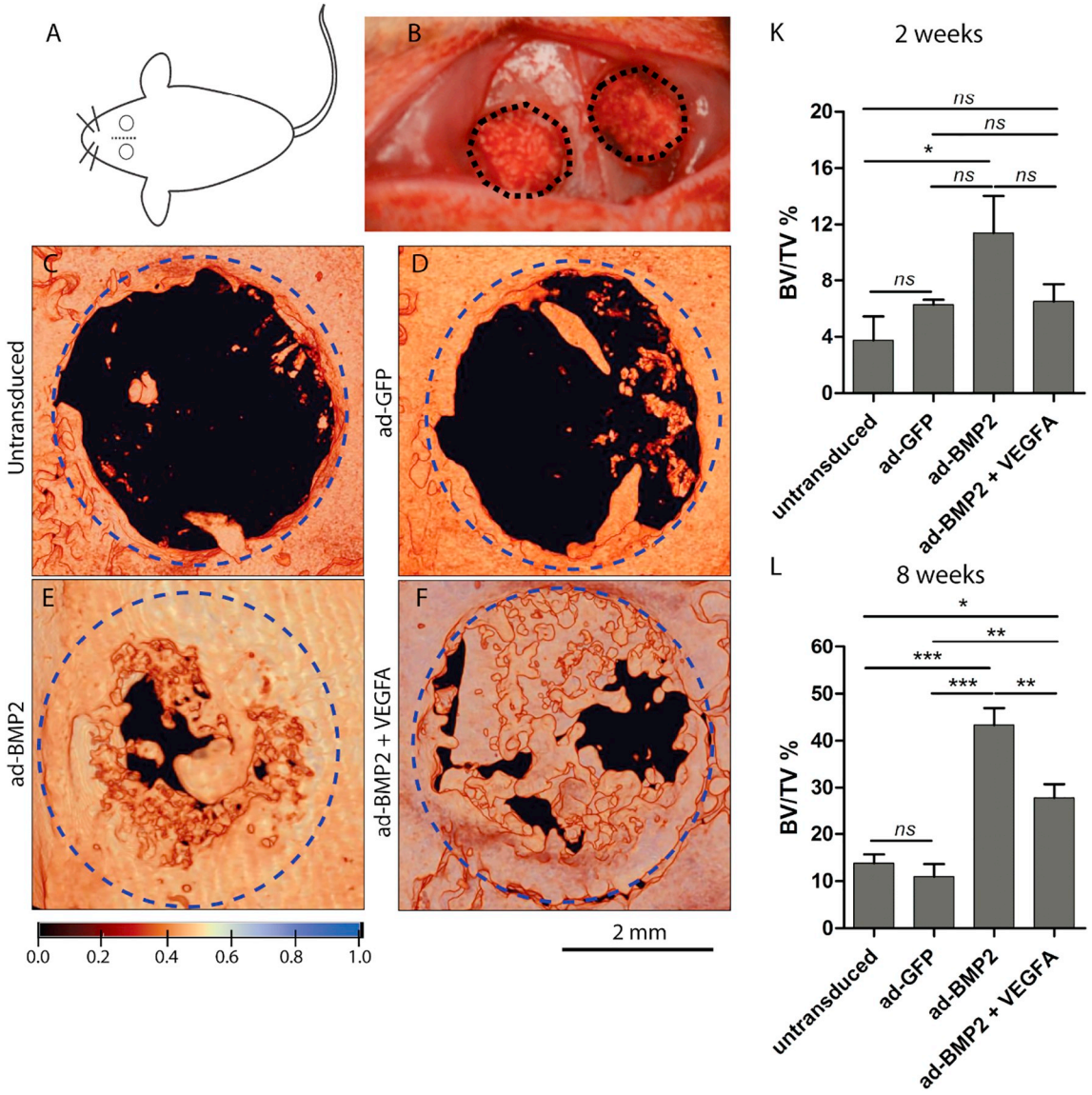

Fig. 3. Expression of BMP2 alone was superior to the combined delivery of BMP2 and VEGFA in formation of radiopaque bone like structures in a critical-sized rat calvarial defect.

Illustration of the location of scaffold implantation sites in rat calvaria and implantation of scaffolds seeded with ad-BMP2, ad-BMP2 + VEGFA, ad-GFP or untransduced rBMSC in rat calvarial bone defects (A and B). At 8 weeks, microCT examination of calvarial defects in the control groups showed few radiopaque bone-like structures (C and D). In contrast, in ad-BMP2 and ad-BMP2 + VEGFA scaffold explants at 8 weeks, abundant radiopaque bone-like areas were observed inside the defect (E and F). Quantification of radiopaque bone like structures in the defects at 2 weeks (K) demonstrated a slightly higher amount of bone formation in ad-BMP2 group, whereas at 8 weeks (L) significantly more bone-like structures were found in ad-BMP2 than in the untransduced, ad-GFP or in the ad-BMP2 + VEGFA group. ANOVA test with Bonferroni *post hoc* analysis was performed for statistical analysis in (K and L). The error bars represent SEM. ***, $p < 0.000$; **, $p = 0.001$ to 0.01;*, $p = 0.01$ to 0.05; ns, non-significant.

intensity of Alizarin staining was weaker in ad-BMP2 + VEGFA group as compared to the ad-BMP2 group (Fig. 2H) which parallels with slightly but significantly lower mRNA levels of *Alpl* and *Runx2* in ad-BMP2 + VEGFA group (Fig. 2A–D).

3.3. Adenoviral mediated delivery of BMP2 alone was superior to the combined delivery of BMP2 + VEGFA in de novo bone formation and healing of a critical sized rat calvarial defect

The ability of BMP2 alone or in combination with VEGFA to induce *de novo* bone formation and healing was investigated by implanting poly(LLA-*co*-CL) scaffold seeded with ad-BMP2, ad-BMP2 + VEGFA, ad-GFP or untransduced rBMSC in critical-sized bone defects in rat calvaria. MicroCT analysis at 8 weeks revealed minimal healing of the defect with few radiopaque bone like structures mostly at the periphery of the defect from untransduced ($n = 8$) and ad-GFP ($n = 8$) explants (Fig. 3C and D). In contrast, all analyzed replicates ($n = 8$) from ad-BMP2 and ad-BMP2 + VEGFA scaffold explants revealed formation of significant amounts of dense bone like structures in the defect area at 8 weeks (Fig. 3E and F). Quantification of new bone formation in the defects showed a significantly higher volume percent (%) of radiopaque structure in ad-BMP2 (43.37 ± 3.55% defect closure), compared with the ad-BMP2 + VEGFA (27.86 ± 2.89% defect closure) and other controls (Fig. 3L). At 2 weeks, formation of the bone like structures was relatively lower in all of the experimental groups, with ad-BMP2 group demonstrating the highest amount of bony structures (Fig. 3K).

To confirm the formation of bony structures disclosed by microCT, histological examination of H & E/Masson's trichrome stained sections

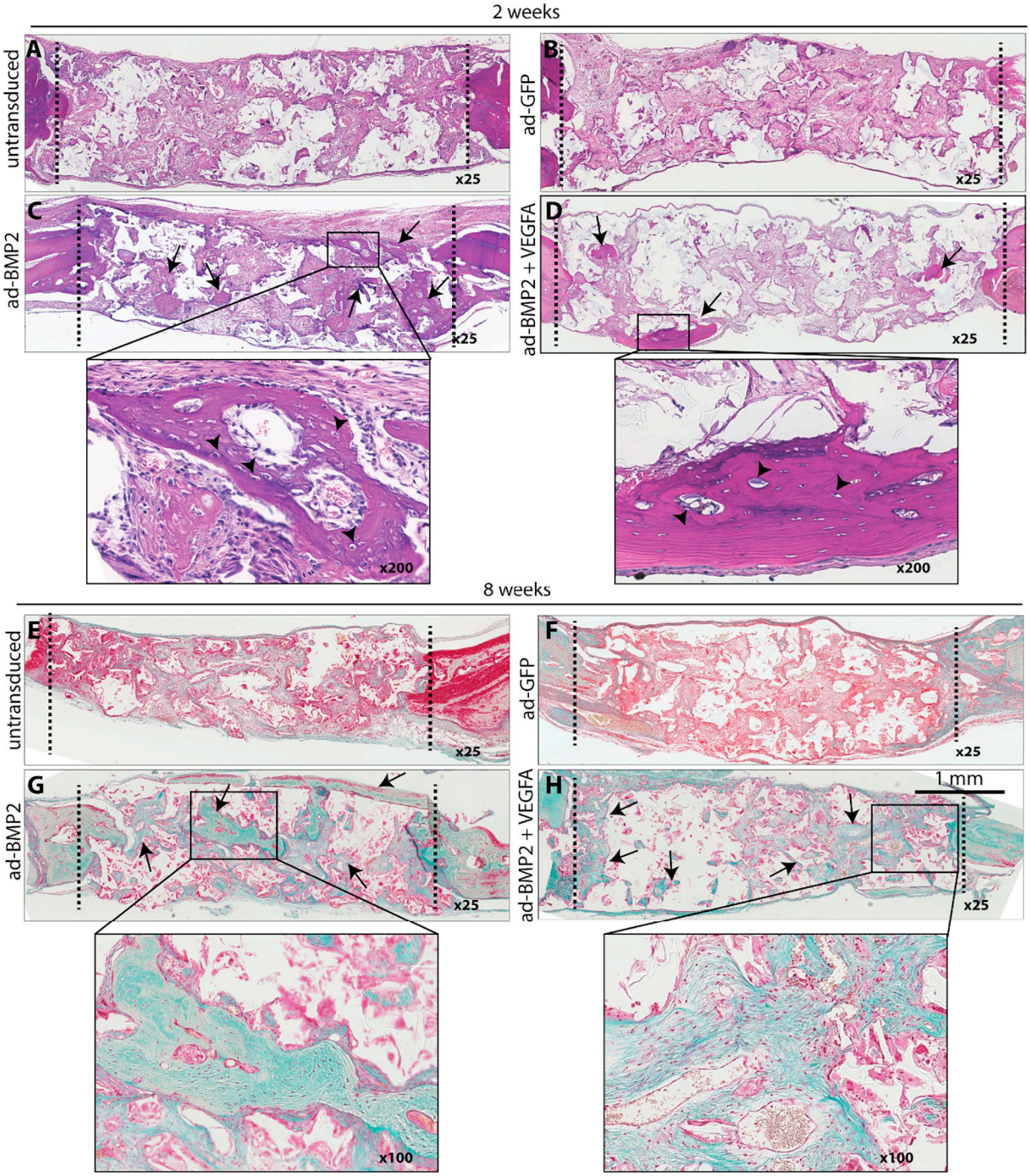

Fig. 4. Expression of BMP2 alone was superior to the combined delivery of BMP2 and VEGFA in formation of vital bony structures in a critical-sized rat calvarial defect.

(A–H) Representative images of H & E/Masson's trichrome stained FFPE sections of scaffold explants from different experimental groups. Apart from the borders of the calvarial defects, formation of bony structures was not obvious in the untransduced and ad-GFP groups both at 2 (A and B, H & E stained slides) and at 8 weeks (E and F, Masson's trichrome stained slides). In both ad-BMP2 (C) and ad-BMP2 + VEGFA (D) groups, formation of bony structures (black arrows) at the borders of the defect (black dotted lines), peripherally and within the scaffold explants was observed as early as 2 weeks. Extensive bone formation (black arrows) with bony trabeculae extending throughout the thickness of the scaffolds was found at 8 weeks in ad-BMP2 (G) and ad-BMP2 + VEGFA (H) groups. Examination of the bony structure at 2 weeks revealed numerous osteocyte-like cells (black arrowheads, inset C and D).

was subsequently undertaken. Similar to the microCT findings, very few bony structures were detected in all replicates of untransduced and ad-GFP groups at both 2 and 8 weeks (Fig. 4A, B, E and F). However, formation of bony structures (black arrows) was detected at the junction of the defect, as well as inside the defects in all replicates in ad-BMP2 and ad-BMP2 + VEGFA groups at 2 weeks (Fig. 4C and D). At 8 weeks, formation of bony structures (blue-green stained areas with black arrows) was more extensive with bony trabeculae extending throughout the whole thickness of the defects (Fig. 4G and H). Bony structure consisted of numerous osteocyte like cells both at 2 (black arrowheads, inset C and D) and 8 (H & E staining not shown for 8 weeks) weeks. Occasional inflammatory and multinucleated giant

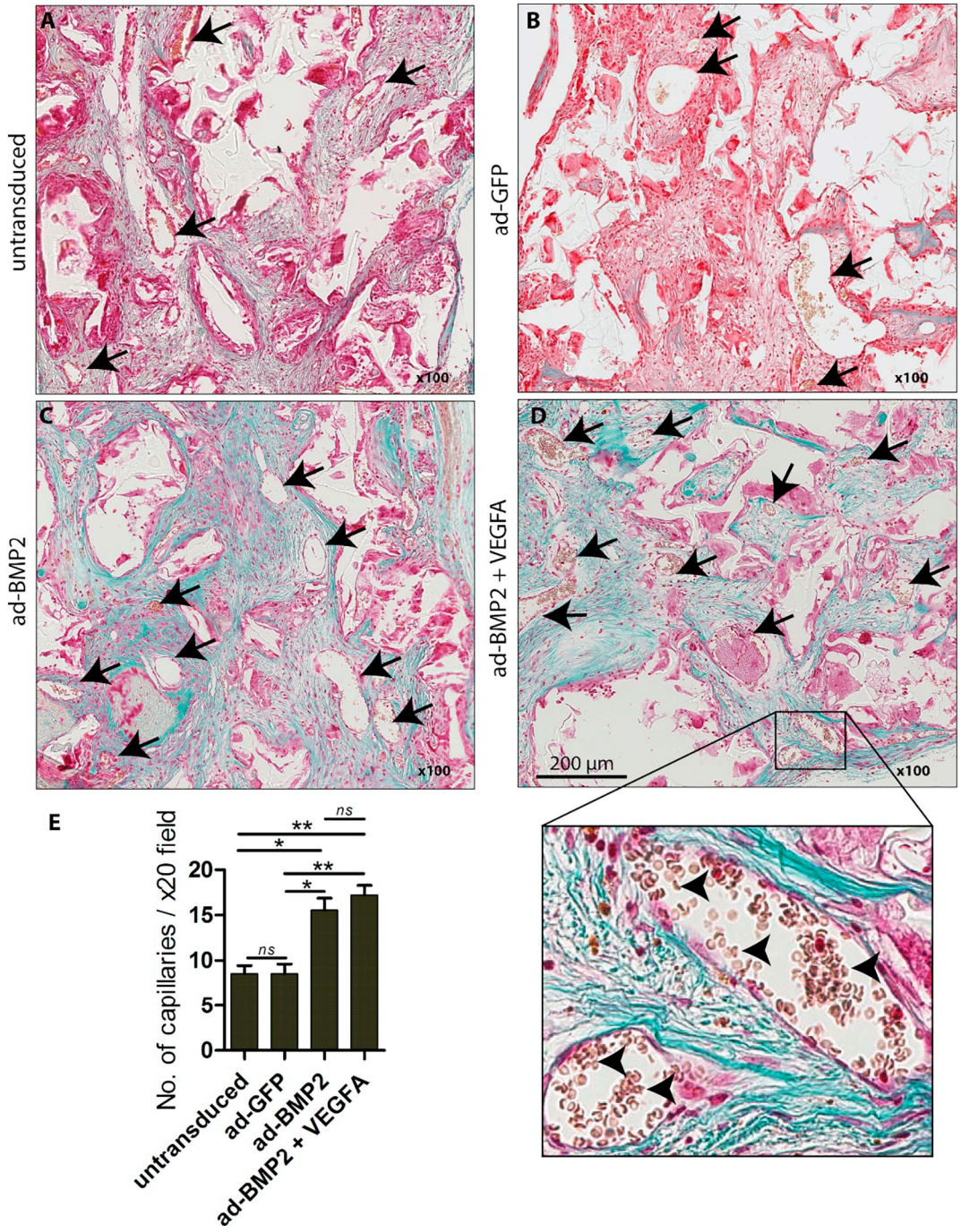

Fig. 5. Adenoviral vector mediated delivery of BMP2 alone or in combination with VEGFA induced formation of capillary like structures in a critical sized rat calvarial bone defect.
(A–D) Representative images of Masson's trichrome stained slides at 8 weeks showing higher numbers of blood capillaries/vessels in ad-BMP2 and ad-BMP2 + VEGFA explants than in the untransduced and ad-GFP explants. Black arrows indicate the pink/red stained capillaries/blood vessels containing brown/orange stained erythrocytes (inset D, arrowheads indicating erythrocytes). (E) Quantification of blood capillaries/vessels demonstrated approximately twice the number in ad-BMP2 and ad-BMP2 + VEGFA, compared with the untransduced and ad-GFP explants. However, no significant difference in the number of blood capillaries/vessels was found between the ad-BMP2 and ad-BMP2 + VEGFA groups. ANOVA test with Bonferroni *post hoc* analysis was performed for statistical analysis in (E). Error bars represent SEM. **, $p = 0.001$ to 0.01;*, $p = 0.01$ to 0.05; ns, non-significant.

cells were seen in all groups. In parallel with the *in vitro* molecular findings and microCT observations, the amount of bone like structure in ad-BMP2 + VEGFA group was lower as compared to that of ad-BMP2 group as observed by H & E/Masson's trichrome analyses (Fig. 4C, D, G and H).

3.4. De novo bone formation in ad-BMP2 and ad-BMP2 + VEGFA rat calvarial explants was associated increased angiogenesis

The association between enhanced bone formation and the degree of angiogenesis in ad-BMP2 and ad-BMP2 + VEGFA scaffold explants was next examined by counting the blood capillaries/vessels in Masson's trichrome stained slides at 8 weeks. Analyses of the scanned

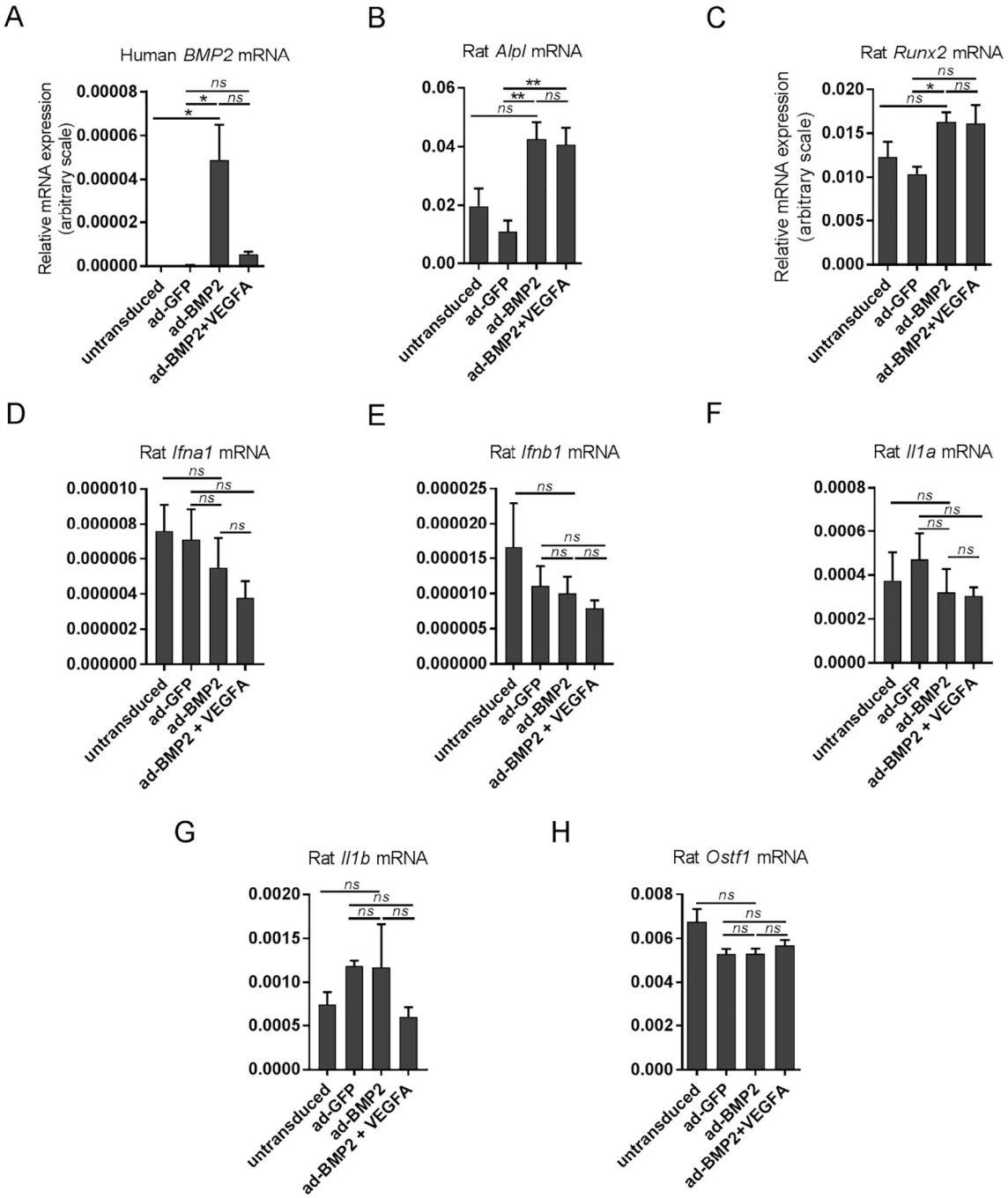

Fig. 6. Delivery of BMP2 alone and in combination with VEGFA was associated with up-regulation of osteogenic markers in the *in vivo* scaffold explants. ANOVA analysis demonstrated up-regulation of human *BMP2* and osteogenesis related rat genes such as *Alpl* and *Runx2* in the ad-BMP2 and ad-BMP2 + VEGFA scaffold explants, compared with the ad-GFP and untransduced explants (A–C). (D–H) Expression levels of innate immunity response genes (*Ifna1*, *Ifnb1*, *Il1a* and *Il1b*) and osteoclast activating factor 1 (*Ostf1*) were similar in the ad-GFP, ad-BMP2 and ad-BMP2 + VEGFA, compared to the untransduced explants. ANOVA test with Bonferroni *post hoc* analysis was performed for statistical analysis. $^{**}p$ = 0.001–0.01, $^{**}p$ = 0.01–0.05, ns = non-significant.

slides showed significantly higher numbers of blood capillaries/vessels in ad-BMP2 and ad-BMP2 + VEGFA rat BMSC explants, compared with the ad-GFP and untransduced controls (Fig. 5A–E). The number of blood capillaries/vessels in ad-BMP2 + VEGFA was slightly but insignificantly higher than in the ad-BMP2 explants (Fig. 5C–E).

3.5. De novo bone formation in ad-BMP2 and ad-BMP2 + VEGFA rat calvarial explants was associated with up-regulation of osteogenic markers

TaqMan qRT-PCR was used to examine the differentially expressed osteogenesis related genes in poly(LLA-*co*-CL) scaffold explants from rat calvarial bone defects at 2 weeks. It was interesting to observe that a higher level of human *BMP2* mRNA from the implanted rat BMSC could still be detected by 2 weeks in the ad-BMP2 and ad-BMP2 + VEGFA scaffold explants (Fig. 6A). Nevertheless, the human *BMP2* mRNA level was much higher in ad-BMP2 compared to the ad-BMP2 + VEGFA scaffold explant (Fig. 6A). However, no human *VEGFA* mRNA could be detected by 2 weeks (data not shown). Osteogenesis related genes such as rat *Alpl* and *Runx2* were found to be up-regulated both in ad-BMP2 and ad-BMP2 + VEGFA, compared with the ad-GFP and untransduced BMSC scaffold explants (Fig. 6B and C).

3.6. Adenoviral delivery of BMP2 alone and in combination with VEGFA was not associated with adverse innate host response in the rat calvarial defect

TaqMan qRT-PCR was used to examine the expression of genes (*Ifna1*, *Ifnb1*, *Il1a* and *Il1b*) related to the innate response to adenoviral infection in the scaffold explants from rat calvarial bone defects at 2 weeks. mRNA expression levels of these genes were similar in ad-GFP, ad-BMP2 and ad-BMP2 + VEGFA explants, compared with the untransduced BMSC explants (Fig. 6D–G). Likewise, mRNA expression of the *Ostf1* (osteoclast stimulating factor 1) was similar in all of the experimental groups (Fig. 6H).

4. Discussion

The critical-sized bone defect model is one of the most extensively applied models for testing the osteogenic potential of growth factors and/or scaffold material using mesenchymal stem cells (Gomes and Fernandes, 2011). The current study tested the effectiveness of adenoviral mediated delivery of human BMP2 alone or in combination with VEGFA in rBMSC, seeded onto a poly(LLA-*co*-CL) scaffolds in bone regeneration. The results showed that the combined delivery of BMP2 and VEGFA did not offer any additional advantage over BMP2 alone in healing the rat calvarial bone defect.

In the current study, the adenoviral mediated delivery of BMP2 and VEGFA was successful (Fig. 1). The increased mRNA expression levels of *BMP2* and *VEGFA* (both human and rat) in rBMSC were associated with the induction of osteogenic marker genes (such as *Alpl* and *Runx2*) and ALP protein in rBMSC seeded onto poly(LLA-*co*-CL) scaffolds at both 3 and 14 days (Fig. 2A–G). Nevertheless, the expression levels of *Alpl* and *Runx2* were moderately but significantly lower in the combined delivery group than in the ad-BMP2 group (Fig. 2A–D). In parallel, the *in vitro* calcium deposition as demonstrated by Alizarin red staining in monolayer and in poly(LLA-*co*-CL) scaffold was lower in ad-BMP2 + VEGFA group (Fig. 2H). These results indicate that delivery of BMP2 alone or in combination with VEGFA was able to differentiate rBMSC seeded onto scaffolds towards an osteogenic pathway, however, the ability of the combined delivery of BMP2 and VEGFA was inferior as compared to the delivery of BMP2 alone. In parallel to these *in vitro* observations, significantly more radiopaque bony structures were detected at 8 weeks in the calvarial bone defects with ad-BMP2, compared with the ad-BMP2 + VEGFA, untransduced and ad-GFP groups (Fig. 3). These observations corroborated with the histological findings of the H & E/Masson's trichrome stained sections, showing formation of more bony structures in the calvarial defects in the ad-BMP2 group, at both 2- and 8 weeks (Fig. 4).

In contrast to these findings, some previous studies have reported an additive effect of the combined delivery of BMP2 and VEGFA (a low ratio of VEGFA to BMP2 as in the current study) on bone formation over the delivery of BMP2 alone (Peng et al., 2005; Zhang et al., 2011). The added benefit of combining VEGFA with BMP2 has been attributed mainly to the indirect effect of VEGFA enhancing angiogenesis and to a lesser extent to the direct effect on osteoblasts (Kempen et al., 2009; Street et al., 2002). In the current study, the reduced bone formation ability of ad-BMP2 + VEGFA was indeed contrary to a slightly higher (but statistically insignificant) number of blood capillaries found in the defect area, compared with the ad-BMP2 group (Fig. 5E). This indicates that the enhanced angiogenesis as observed in ad-BMP2 + VEGFA group was not able to complement the osteogenic ability of BMP2 alone. It may be argued that the reduced bone formation in ad-BMP2 + VEGFA could be due to the slightly lower amount of ad-BMP2 virus particles used (80 MOI as compared with the 100 MOI used in the ad-BMP2 group) in the combined delivery group. A dose dependent reduction in new bone formation (a reduction of almost 50% bone volume with 50% reduction in rhBMP2 amount) has been reported previously for recombinant BMP2 in a rat calvarial bone defect model (Young et al., 2009). Nevertheless, a higher degree of reduction in bone formation (27.86% BV/TV bone formation for ad-BMP2 + VEGFA *versus* 43.37% for ad-BMP2) in the combined group cannot be solely attributed to 20% reduction in the amount of ad-BMP2 virus particles. This indicates that other mechanisms might also have contributed to the reduced bone formation in the combined group. Inclusion of 1:4 ratio of ad-GFP and ad-BMP2 as an additional control might have been helpful to clarify this issue.

Schönmeyr B et al. have demonstrated that the adenoviral medicated delivery of VEGFA was able to inhibit significantly the expression BMP2 when VEGFA and BMP2 were co-expressed, or uni-transfected rat BMSC cells were co-cultured (Schönmeyr et al., 2009). This could be the more likely explanation for reduced ability of the ad-BMP2 + VEGFA group because similar methods were used in the current study. Other possible explanations could be the inhibition of BMP2 mediated osteoblastic differentiation by VEGFA (Lin et al., 2014) (Song et al., 2011), dilution of the number of stem cells available for osteogenic differentiation by favoring their differentiation towards the endothelial lineage (Peng et al., 2002), or inhibition of endothelial to mesenchymal transition (Hu et al., 2017). Additionally, VEGFA has been shown to promote osteoclast recruitment in the osteogenic grafts, thereby indirectly leading to bone resorption and reduced bone volume (Helmrich et al., 2013). In the current study, this possibility is less likely as the expression of *Ostf1* (osteoclast stimulating factor 1) was similar both in the combined delivery group and ad-BMP2 group.

Peng H et al. have reported that VEGFA was able to enhance cellular survival at the bone regeneration site when combined with BMP4 (Peng et al., 2002). However, the ability of VEGFA to support cell survival appears to be dependent on cell type. In fact it has been reported that adenoviral mediated co-expression of VEGFA and BMP4 resulted in reduced proliferative ability of C2C12 cells compared with the expression of BMP4 alone (Li et al., 2009). It was interesting to note that by 2 weeks, no human *VEGFA* mRNA was detected in the scaffold implants at the defect site in all of the groups (data not shown), although higher expression of human BMP2 was found in the ad-BMP2 group (Fig. 6A). This could be due to the selective cell death or differentiation of rBMSC co-expressing BMP2 and VEGFA at the defect site and warrants further investigation.

In conclusion, the current study tested the feasibility of a recently established model system (poly(LLA-*co*-CL) scaffold + BMSC transduced with adenoviral particles) (Sharma et al., 2016; Sharma et al., 2018) for bone regeneration using a more clinically relevant critical sized rat calvarial bone defect model and demonstrated that the delivery of BMP2 alone or in combination with VEGFA was not associated with adverse host response. More importantly, the delivery of BMP2 alone was more efficient as compared to the combined delivery of BMP2 and VEGFA in bone regeneration. However, the positive effects of VEGFA on angiogenesis cannot be denied and it highlights the importance of selecting appropriate growth factors and correct formulation strategies for successful bone regeneration in the model system used in the current study.

Declaration of interest

None.

Transparency document

The Transparency document associated with this article can be found, in online version.

Acknowledgements

We are thankful to Randi Sundfjord for the technical assistance (histological sectioning and staining) and Dr. Joan Bevenius for English language revision of the manuscript. We greatly acknowledge the

financial support of the Meltzer Research Fund, The European Union FP7,VascuBone (Project number 242175) and Helse Vest project (Project number 502027 and 912048).

References

Avivi, A., Resnick, M.B., Nevo, E., Joel, A., Levy, A.P., 1999. Adaptive hypoxic tolerance in the subterranean mole rat Spalax ehrenbergi: the role of vascular endothelial growth factor. FEBS Lett. 452 (3), 133–140.

Danmark, S., Finne-Wistrand, A., Wendel, M., Arvidson, K., Albertsson, A., Mustafa, K., 2010. Osteogenic differentiation by rat bone marrow stromal cells on customized biodegradable polymer scaffolds. J. Boact. Compat. Pol. 25, 207–223.

Dånmark, S., Finne-Wistrand, A., Schander, K., Hakkarainen, M., Arvidson, K., Mustafa, K., Albertsson, A.C., 2011. In vitro and in vivo degradation profile of aliphatic polyesters subjected to electron beam sterilization. Acta Biomater. 7 (5), 2035–2046.

Evans, C.H., 2012. Gene delivery to bone. Adv. Drug Deliv. Rev. 64 (12), 1331–1340.

Ferrara, N., 2002. VEGF and the quest for tumour angiogenesis factors. Nat. Rev. Cancer 2 (10), 795–803.

Fillingham, Y., Jacobs, J., 2016. Bone grafts and their substitutes. Bone Joint J. 98-b (1 Suppl A), 6–9.

Freire, M.O., Kim, H.K., Kook, J.-K., Nguyen, A., Zadeh, H.H., 2012. Antibody-mediated osseous regeneration: the early events in the healing response. Tissue Eng. A 19 (9–10), 1165–1174.

Freire, M., Choi, J.-H., Nguyen, A., Chee, Y.D., Kook, J.-K., You, H.-K., Zadeh, H.H., 2015. Application of AMOR in craniofacial rabbit bone bioengineering. Biomed. Res. Int. 2015, 7.

Gomes, P.S., Fernandes, M.H., 2011. Rodent models in bone-related research: the relevance of calvarial defects in the assessment of bone regeneration strategies. Lab. Anim. 45 (1), 14–24.

Helmrich, U., Di Maggio, N., Güven, S., Groppa, E., Melly, L., Largo, R.D., Heberer, M., Martin, I., Scherberich, A., Banfi, A., 2013. Osteogenic graft vascularization and bone resorption by VEGF-expressing human mesenchymal progenitors. Biomaterials 34 (21), 5025–5035.

Hu, K., Besschetnova, T.Y., Olsen, B.R., 2017. Soluble VEGFR1 reverses BMP2 inhibition of intramembranous ossification during healing of cortical bone defects. 35 (7), 1461–1469.

Idris, S.B., Dånmark, S., Finne-Wistrand, A., Arvidson, K., Albertsson, A.-C., Bolstad, A.I., Mustafa, K., 2010. Biocompatibility of polyester scaffolds with fibroblasts and osteoblast-like cells for bone tissue engineering. J. Bioact. Compat. Polym. 25 (6), 567–583.

Kempen, D.H.R., Lu, L., Heijink, A., Hefferan, T.E., Creemers, L.B., Maran, A., Yaszemski, M.J., Dhert, W.J.A., 2009. Effect of local sequential VEGF and BMP-2 delivery on ectopic and orthotopic bone regeneration. Biomaterials 30 (14), 2816–2825.

Li, G., Corsi-Payne, K., Zheng, B., Usas, A., Peng, H., Huard, J., 2009. The dose of growth factors influences the synergistic effect of vascular endothelial growth factor on bone morphogenetic protein 4–induced ectopic bone formation. Tissue Eng. A 15 (8), 2123–2133.

Li, B., Wang, H., Qiu, G., Su, X., Wu, Z., 2016. Synergistic effects of vascular endothelial growth factor on bone morphogenetic proteins induced bone formation in vivo: influencing factors and future research directions. Biomed. Res. Int. 2016, 2869572.

Lin, Z., Wang, J.-S., Lin, L., Zhang, J., Liu, Y., Shuai, M., Li, Q.I., 2014. Effects of BMP2 and VEGF165 on the osteogenic differentiation of rat bone marrow-derived mesenchymal stem cells. Exp. Ther. Med. 7 (3), 625–629.

Maniatopoulos, C., Sodek, J., Melcher, A.H., 1988. Bone formation in vitro by stromal cells obtained from bone marrow of young adult rats. Cell Tissue Res. 254 (2), 317–330.

Odelius, K., Plikk, P., Albertsson, A., 2005. Elastomeric hydrolyzable porous scaffolds: copolymers of aliphatic polyesters and a polyether-ester. Biomacromolecules 6, 2718–2725.

Park, J., Ries, J., Gelse, K., Kloss, F., von der Mark, K., Wiltfang, J., Neukam, F.W., Schneider, H., 2003. Bone regeneration in critical size defects by cell-mediated BMP-2 gene transfer: a comparison of adenoviral vectors and liposomes. Gene Ther. 10 (13), 1089–1098.

Peng, H., Wright, V., Usas, A., Gearhart, B., Shen, H.-C., Cummins, J., Huard, J., 2002. Synergistic enhancement of bone formation and healing by stem cell–expressed VEGF and bone morphogenetic protein-4. J. Clin. Invest. 110 (6), 751–759.

Peng, H., Usas, A., Olshanski, A., Ho, A.M., Gearhart, B., Cooper, G.M., Huard, J., 2005. VEGF improves, whereas sFlt1 inhibits, BMP2-induced bone formation and bone healing through modulation of angiogenesis. J. Bone Miner. Res. 20 (11), 2017–2027.

Schönmeyr, B.H., Soares, M., Avraham, T., Clavin, N.W., Gewalli, F., Mehrara, B.J., 2009. Vascular endothelial growth factor inhibits bone morphogenetic protein 2 expression in rat mesenchymal stem cells. Tissue Eng. A 16 (2), 653–662.

Sharma, S., Sapkota, D., Xue, Y., Sun, Y., Finne-Wistrand, A., Bruland, O., Mustafa, K., 2016. Adenoviral mediated expression of BMP2 by bone marrow stromal cells cultured in 3D copolymer scaffolds enhances bone formation. PLoS One 11 (1), e0147507.

Sharma, S., Sapkota, D., Xue, Y., Rajthala, S., Yassin, M.A., Finne-Wistrand, A., Mustafa, K., 2018. Delivery of VEGFA in bone marrow stromal cells seeded in copolymer scaffold enhances angiogenesis, but is inadequate for osteogenesis as compared with the dual delivery of VEGFA and BMP2 in a subcutaneous mouse model. Stem Cell Res Ther 9 (1), 23.

Song, X., Liu, S., Qu, X., Hu, Y., Zhang, X., Wang, T., Wei, F., 2011. BMP2 and VEGF promote angiogenesis but retard terminal differentiation of osteoblasts in bone regeneration by up-regulating Id1. Acta Biochim. Biophys. Sin. 43 (10), 796–804.

Street, J., Bao, M., deGuzman, L., Bunting, S., Peale, F.V., Ferrara, N., Steinmetz, H., Hoeffel, J., Cleland, J.L., Daugherty, A., et al., 2002. Vascular endothelial growth factor stimulates bone repair by promoting angiogenesis and bone turnover. Proc. Natl. Acad. Sci. 99 (15), 9656–9661.

Xing, Z., Xue, Y., Danmark, S., Schander, K., Ostvold, S., Arvidson, K., Hellem, S., Finne-Wistrand, A., Albertsson, A., Mustafa, K., 2011. Effect of endothelial cells on bone regeneration using poly(ι-lactide-co-1,5-dioxepan-2-one) scaffolds. J. Biomed. Mater. Res. A 96, 349–357.

Xue, Y., Danmark, S., Xing, Z., Arvidson, K., Albertsson, A.C., Hellem, S., Finne-Wistrand, A., Mustafa, K., 2010. Growth and differentiation of bone marrow stromal cells on biodegradable polymer scaffolds: an in vitro study. J. Biomed. Mater. Res. A 95 (4), 1244–1251.

Young, S., Patel, Z.S., Kretlow, J.D., Murphy, M.B., Mountziaris, P.M., Baggett, L.S., Ueda, H., Tabata, Y., Jansen, J.A., Wong, M., et al., 2009. Dose effect of dual delivery of vascular endothelial growth factor and bone morphogenetic protein-2 on bone regeneration in a rat critical-size defect model. Tissue Eng. Part A 15 (9), 2347–2362.

Younger, E.M., Chapman, M.W., 1989. Morbidity at bone graft donor sites. J. Orthop. Trauma 3 (3), 192–195.

Zhang, W., Wang, X., Wang, S., Zhao, J., Xu, L., Zhu, C., Zeng, D., Chen, J., Zhang, Z., Kaplan, D.L., et al., 2011. The use of injectable sonication-induced silk hydrogel for VEGF165 and BMP-2 delivery for elevation of the maxillary sinus floor. Biomaterials 32 (35), 9415–9424.